

Ferromagnetic Interaction in $\mu_{1,3}$ -Cyanamido-Derived Copper(II) Cryptates

Albert Escuer,^[a] Vickie Mc Kee,^[b] Jane Nelson,^[c] Eliseo Ruiz,^[a, d] Núria Sanz,^[a] and Ramon Vicente*^[a]

Abstract: The reaction of dinuclear copper(II) cryptates with calcium cyanamide, CaNCN, and sodium dicyanamide, Na[N(CN)₂] results in dinuclear compounds of formulae [Cu₂(HNCN)(R3Bm)](ClO₄)₃ (**1**), [Cu₂(dca)(R3Bm)](ClO₄)₃·4H₂O (**2**), and [Cu₂(NCNCONH₂)(R3Bm)](CF₃SO₃)₃ (**3**), in which R3Bm = N[(CH₂)₂-NHCH₂(C₆H₄-*m*)CH₂NH(CH₂)₂]₃N and dca = dicyanamido ligand (NCNCN⁻).

The X-ray diffraction analysis reveals for both **1** and **3** a dinuclear entity in which the copper atoms are bridged by means of the -NCN- unit. The molar magnetic susceptibility measurements

of **1–3** in the 2–300 K range indicate ferromagnetic coupling. The calculated *J* values, by using theoretical methods based on density functional theory (DFT) are in excellent agreement with the experimental data. Catalytic hydration of a nitrile to an amide functional group is assumed responsible for the formation of **3** from a $\mu_{1,3}$ -dicyanamido ligand.

Keywords: copper • density functional calculations • magnetic properties • N ligands • structure elucidation

Introduction

Pseudohalide-linked assemblies^[1] represent one of the most intensively studied groups of bridged assemblies, particularly in respect of their magnetic properties. This is because the rich variety of coordination linkage options they offer is mirrored by a matching variety of magnetic interaction pathways. In most cases the magnetic interaction transmitted in the various available bridging modes is significantly affected by the geometry around the bridge. With the symmetric azido linker,^[2,3] the consequence of this interaction ranges

from effective magnetic silence in some noncolinear 1,3-linked dimetallic systems^[4] to ferromagnetic coupling in 1,1- and colinear 1,3-arrangements.^[5,6] In cases in which the bridging pseudohalide is unsymmetrical, the options for coordination linkage and associated magnetic interaction pathways are further increased.^[3b]

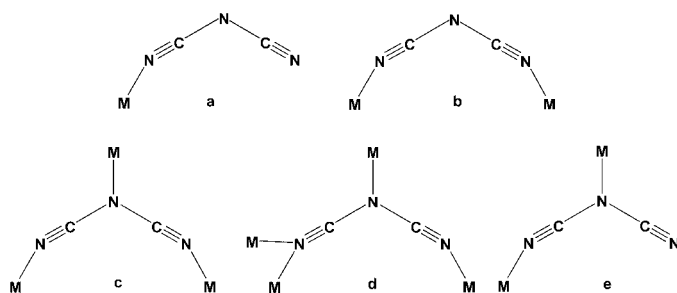
Despite the considerable attention given to polynuclear bridging N₃⁻ systems,^[2] the isoelectronic cyanamido analogue, NCN²⁻, or the protonated hydrogencyanamido group, NCNH⁻, have attracted minimal interest. We know of only one report of magnetic interaction mediated by a hydrogencyanamido-derived link;^[7a] this relates to a doubly-bridged hydrogencyanamido dicopper(II) assembly accidentally generated in the course of a thiourea desulfurisation reaction. (A dinickel μ -hydrogencyanamido complex of dipodand amine ligand^[7b] has been recently synthesised, but no magnetic results are available for this compound.) On the other hand, the versatile dicyanamido NCNCN⁻ linker (Scheme 1) has been widely studied for its ability to generate one-, two- and three-dimensional derivatives with interesting magnetic properties.^[8] This ligand can operate as terminal- (**a**), in $\mu_{1,5}$ - (**b**), $\mu_{1,3,5}$ - (**c**), and $\mu_{1,1',3,5}$ -bridging (**d**) modes. The $\mu_{1,3}$ -bridging mode (**e**), has been only observed in a polynuclear copper(II) compound with two differing Cu–N(dicyanamido) coordinate bond lengths, for which one Cu–N_{dicyanamido} bond is no more than hemicoordinate. In consequence, the dicyanamido ligand does not act as a bridge, and fails to transmit magnetic interactions.^[9] On the other hand, the existence of

[a] Prof. A. Escuer, Dr. E. Ruiz, Dr. N. Sanz, Dr. R. Vicente
Departament de Química Inorgànica
Universitat de Barcelona, c. Martí i Franquès 1–11
08028 Barcelona (Spain)
Fax: (+34) 934-907-725
E-mail: ramon.vicente@qi.ub.es

[b] Prof. V. Mc Kee
Department of Chemistry, Loughborough University
Loughborough, LE11 3TU (UK)

[c] Prof. J. Nelson
Biomolecular Sciences, University of Ulster
Cromore Rd Coleraine, BT52 1SA (UK)

[d] Dr. E. Ruiz
Centre de Recerca en Química Teòrica
Universitat de Barcelona, Diagonal 647
08028 Barcelona (Spain)



Scheme 1.

phenylcyanamide derivatives^[10] and their capacity for bridging^[11] has been known for some time, but the first magnetic measurements on these systems have been only recently reported for a series of polynuclear manganese(II) complexes.^[12] These in general show antiferromagnetic coupling somewhat weaker than in the azido analogues.

Given the scarcity of magnetic studies of 1,3-linked cyanamido-derived systems and the possible importance of the 1,3-pathway in the dicyanamide systems, we undertook the synthesis of dinuclear –NCN–linked derivatives by using a strategy well-established for azido^[6] and other triatomic^[13] bridging units. This involves the use of aminocryptand ligands to supply a pair of appropriately (5–6 Å) separated N4-cap coordination sites to attract and retain transition-metal ions, which then (fully or partially) complete their coordination sphere by insertion of an axially disposed bridging ligand.^[14] Within the range of cryptate hosts studied, single mono-, bi- and triatomic bridges can be accommodated; the *m*-xylyl linked cryptand R3Bm has been shown to offer the best fit for triatomic bridges.

Results and Discussion

Synthesis of complexes:

$[Cu_2(HNCN)(R3Bm)](ClO_4)_3$ (**1**): The affinity of Cu^{II} for additional ligation is shown in the ready acquisition of bridging hydrogencyanamido, HNCN[–], ligands in a heterogeneous reaction between calcium cyanamide and a solution of the dicopper(II) cryptate $[Cu_2(R3Bm)]^{4+}$.

IR spectroscopy shows a single, moderately strong, asymmetric-stretching absorption ν_{as} around 2200 cm^{–1} for the hydrogencyanamido ligand, shifted somewhat to low frequency relative to its uncoordinated protonated parent^[15] and considerably to high frequency of the absorption in the bent doubly bridged geometry:^[7] a pattern familiar from the spectroscopic behaviour of the azido series.^[16] As in the case of azido cryptates, the symmetric stretch falls in the region of cryptand fingerprint absorption and cannot be reliably assigned. Crystals of **1**·MeCN·MeOH suitable for X-ray diffraction were obtained by vapor diffusion of MeOH into a solution of the perchlorate salt of the copper(II) cryptate cyanamide complex in MeCN.

$[Cu_2(dca)(R3Bm)](ClO_4)_3 \cdot 4H_2O$ (**2**): Having synthesised the dimeric, bridging hydrogencyanamido derivative, we studied the dicyanamido link. A similar synthetic procedure was used, substituting Ca(NCN) for Na[N(CN)₂].

From the analytical and IR data we assign the formula $[Cu_2(dca)(R3Bm)](ClO_4)_3 \cdot 4H_2O$ (dca = dicyanamido) to product **2**. From consideration of the steric requirements, we assume that the dicyanamido ligand acts as a bridging ligand between the two copper(II) atoms in the 1,3-mode.

$[Cu_2(NCNCNH_2)(R3Bm)](CF_3SO_3)_3$ (**3**): Complex **2** could not be satisfactorily recrystallised on account of the low solubility of the perchlorate salt, so the synthetic procedure was repeated with the more soluble triflate cryptate salt.

Slow crystallisation in this case produced blue-green crystals of **3**·0.5EtOH·0.5H₂O with a simple ν_{as} absorption at 2228 cm^{–1} and a new moderately intense band at 1663 cm^{–1} in the carbonyl stretching region, together with enhanced intensity and complexity in the NH stretching region. X-ray crystallographic examination of this product readily explains the origin of the spectroscopic modifications. The dicyanamido link NCNCN[–] has been changed to the corresponding amido NCNCNH₂[–], presumably through catalytic hydrolysis of the uncoordinated –CN link following attack by H₂O, activated by coordination to the Lewis acidic Cu^{II} ion. Consequently the IR spectrum demonstrates the presence of new CO and NH₂ absorptions, as well as simplification of the 2300–2100 cm^{–1} cyanamido region deriving from substitution of a single coupled NCN oscillator for the more complex NCNCN system.

It is apparent that long-term residence in solution has resulted in alteration of the dicyanamido entity. As this reaction has not been mentioned by other researchers in the dicyanamido field,^[8] we suspect it may be explained by the coordination of the dicyanamido ligand in a “cascade” fashion to the pair of cations encapsulated by the azacryptand: the secondary coordination of anionic or other bridges between the cations themselves coordinated by a cryptand host molecule was termed *cascade* coordination^[17] quite some time ago, in the implicit expectation that the bridging groups might be activated toward further chemical reaction.^[13,14,17] Catalytic hydration of nitriles is not unknown; indeed the dinickel salt of the pseudocryptand dipodand host mentioned above has been recognised as a potent catalyst in the cooperative hydration of nitriles.^[7b] The activation of the β -carbon atom of the dicyanamido ligand by coordination to Cu^{II} against the reaction with methanol has also been reported.^[18] A recent communication,^[19] the results of which, however, we have been unable to replicate,^[20] reports quantitative conversion of MeCN to CN[–] within the analogous *p*-xylene spaced dicopper cryptate.

Description of structures:

$[Cu_2(HNCN)(R3Bm)](ClO_4)_3 \cdot MeCN \cdot MeOH$ (**1**·MeCN·MeOH): A view of the cation is presented in Figure 1 and selected bond lengths and angles are listed in Table 1. The

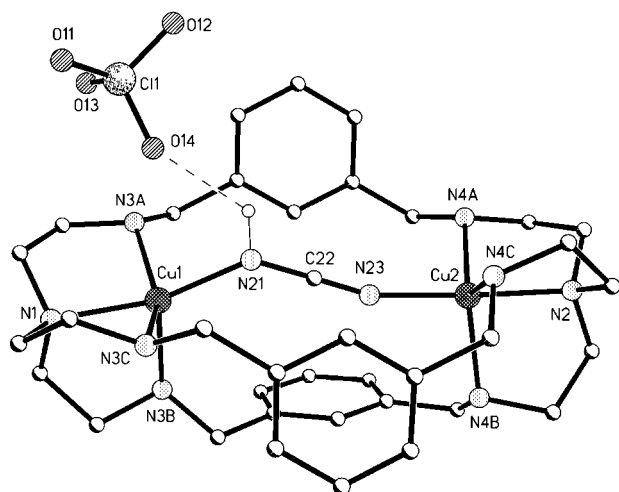


Figure 1. Labeled plot of the cationic unit $[\text{Cu}_2(\text{HNCN})(\text{R3Bm})]^{3+}$ in **1**.

Table 1. Selected bond lengths [Å] and angles [°] for **1**-MeCN-MeOH.^[a]

Cu1–N21	1.968(4)	Cu2–N23	1.925(4)	
Cu1–N1	2.072(4)	Cu2–N2	2.047(4)	
Cu1–N3A	2.105(4)	Cu2–N4A	2.125(4)	
Cu1–N3C	2.111(4)	Cu2–N4C	2.144(4)	
Cu1–N3B	2.255(4)	Cu2–N4B	2.157(4)	
N21–C22	1.290(6)	C22–N23	1.161(6)	
N21–Cu1–N1	163.73(15)	N23–Cu2–N2	176.64(16)	
N21–Cu1–N3A	91.56(15)	N23–Cu2–N4A	93.77(15)	
N1–Cu1–N3A	83.48(16)	N2–Cu2–N4A	84.97(15)	
N21–Cu1–N3C	93.90(15)	N23–Cu2–N4C	94.29(16)	
N1–Cu1–N3C	82.18(15)	N2–Cu2–N4C	83.74(16)	
N3A–Cu1–N3C	146.70(15)	N4A–Cu2–N4C	121.22(15)	
N21–Cu1–N3B	113.33(15)	N23–Cu2–N4B	98.76(16)	
N1–Cu1–N3B	82.91(15)	N2–Cu2–N4B	84.54(15)	
N3A–Cu1–N3B	102.92(14)	N4A–Cu2–N4B	120.72(15)	
N3C–Cu1–N3B	104.90(14)	N4C–Cu2–N4B	115.25(15)	
C22–N21–Cu1	136.3(3)	C22–N23–Cu2	160.5(4)	
N23–C22–N21	179.3(5)			
Hydrogen bonds				
D–H...A	<i>d</i> (D–H)	<i>d</i> (H...A)	<i>d</i> (D...A)	∠(DHA)
N3A–H3A...O13	0.90	2.38	3.129(6)	140.9
N3A–H3A...O14	0.90	2.41	3.168(5)	142.1
N3B–H3B...O21	0.90	2.39	3.146(6)	140.8
N3C–H3C...N31	0.90	2.43	3.228(7)	148.1
N4A–H4A...O11 #1	0.90	2.32	3.156(6)	155.3
N4A–H4A...O61 #2	0.90	2.59	3.150(11)	120.6
N4B–H4B...O22 #3	0.90	2.59	3.209(6)	126.6
N4C–H4C...O12 #1	0.90	2.38	3.263(7)	166.3
N21–H21...O14	0.97	2.30	3.003(5)	128.9

[a]Symmetry transformations used to generate equivalent atoms: #1: $-x+1, -y+1, -z$; #2: $-x+3/2, y+1/2, -z+1/2$; #3: $-x+3/2, y-1/2, -z+1/2$.

structure of the cation confirms the -NCN- bridge with different Cu–N–C angles (Cu1–N21–C22 and C22–N23–Cu2 136.3(3) and 160.5(4)°, respectively). Both Cu^{II} ions are five-coordinate, one in approximately square-pyramidal geometry^[21] (trigonality index, $\tau=0.28$ for Cu1) and the other centering a near-regular trigonal bipyramid ($\tau=0.92$). The

bridging link is well localised, with one short (C22–N23, 1.161(6) Å) and one long (N21–C22, 1.290(6) Å) bond. The N23 atom involved in the shorter bond coordinates the Cu^{II} ion in the trigonal-bipyramidal environment and that involved in the longer one, N21, the Cu^{II} ion in the irregular square-pyramidal environment. The proton of the cyanamido bridge makes a weak N–H...O(ClO₃) hydrogen bond (N21...O14#3 = 3.003(5) Å). The overall distance between the paramagnetic centres (6.024 Å) compares well with that in the azido analogue (6.027 Å),^[14] as do the relatively short Cu–N distances (Cu1–N21, 1.968(4) and Cu2–N23, 1.925(4) Å). The overall conformation of the cryptate, a parallel disposition of two of the xylyl rings with the third lying mutually perpendicular, is also similar to that found in the azido systems. There are some longish (3.5–3.7 Å) intermolecular π – π contacts, as found in the analogous azido-bridged cryptates. In comparison with the relatively unconstrained dinickel μ -hydrogencyanamido complex mentioned earlier,^[7b] which has N–C bond lengths of 1.176 and 1.286 Å, together with an N–H...O(ClO₃) hydrogen bond of 3.035 Å, the cyanamido bridge in **1** is less delocalised toward the pseudoallylic resonance form. All of the cryptand amine protons are involved in weak hydrogen-bonding interactions with anions or solvate molecules.

$[\text{Cu}_2(\text{NCNCONH}_2)(\text{R3Bm})](\text{CF}_3\text{SO}_3)_3 \cdot 0.5 \text{EtOH} \cdot 0.5 \text{H}_2\text{O}$ (**3**·0.5 EtOH·0.5 H₂O): A view of the cation is presented in Figure 2 and selected bond lengths and angles are listed in

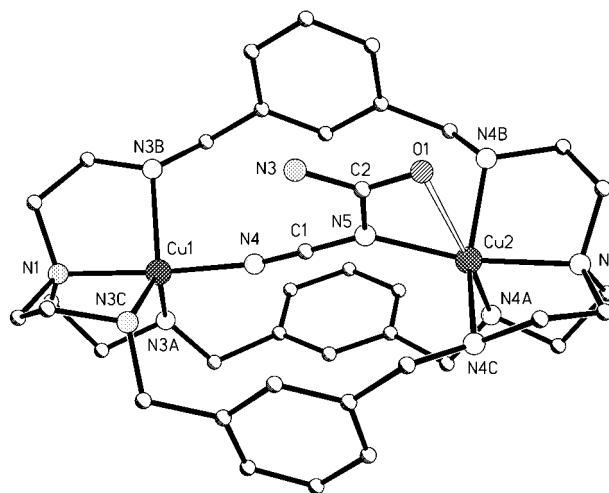


Figure 2. Labeled plot of the cationic unit $[\text{Cu}_2(\text{NCNCONH}_2)(\text{R3Bm})]^{3+}$ in **3**.

Table 2. The structure of the cation demonstrates the consequences of bridge asymmetry, in that one atom (Cu1) is near five-coordinate square-pyramidal ($\tau=0.15$), while the other approaches six-coordinate geometry, following hemicoordination of the amidic O1 atom at 2.714(5) Å. As before the shortest Cu–N distances are those involving the 1,3-cyanamido bridge (Cu1–N4, 1.947(7); Cu2–N5, 2.040(6) Å), which again shows localised bonding: one short

Table 2. Selected bond lengths [Å] and angles [°] for 3·0.5EtOH·0.5-H₂O.^[a]

Cu1–N4	1.947(7)	Cu2–N2	2.082(6)	
Cu1–N1	2.033(6)	Cu2–N4C	2.094(5)	
Cu1–N3C	2.087(5)	Cu2–N4A	2.282(5)	
Cu1–N3B	2.124(6)	Cu1–N3A	2.148(6)	
C1–N5	1.323(9)	N4–C1	1.156(8)	
C2–O1	1.209(8)	N5–C2	1.415(9)	
Cu2–N5	2.040(6)	C2–N3	1.333(9)	
Cu2–N4B	2.077(5)			
N4–Cu1–N1	174.6(2)	N5–Cu2–N4B	90.2(2)	
N4–Cu1–N3C	93.4(2)	N5–Cu2–N2	159.1(2)	
N1–Cu1–N3C	84.9(2)	N4B–Cu2–N2	83.9(2)	
N4–Cu1–N3B	92.2(2)	N5–Cu2–N4C	93.2(2)	
N1–Cu1–N3B	84.8(2)	N4B–Cu2–N4C	150.3(2)	
N3C–Cu1–N3B	127.3(2)	N2–Cu2–N4C	82.5(2)	
N4–Cu1–N3A	102.6(2)	N5–Cu2–N4A	119.2(2)	
N1–Cu1–N3A	82.6(2)	N4B–Cu2–N4A	100.6(2)	
N3C–Cu1–N3A	124.4(3)	N2–Cu2–N4A	81.7(2)	
N3B–Cu1–N3A	105.2(3)	N4C–Cu2–N4A	103.4(2)	
C1–N4–Cu1	161.4(5)	C2–N5–Cu2	107.5(5)	
N4–C1–N5	178.7(7)	O1–C2–N3	124.2(7)	
C1–N5–C2	117.4(6)	O1–C2–N5	116.7(6)	
C1–N5–Cu2	135.1(5)	N3–C2–N5	118.9(7)	
Hydrogen bonds				
D–H...A	d(D–H)	d(H...A)	d(D...A)	∠(DHA)
N3A–H3A...O13 #1	0.93	2.49	3.404(13)	165.8
N4A–H4A...O31 #1	0.93	2.31	3.159(8)	152.1
N3B–H3B...O21	0.93	2.19	3.000(8)	144.6
N4B–H4B...O1	0.93	2.29	2.914(7)	123.6
N3C–H3C...O11 #2	0.93	2.29	2.966(8)	129.1
N4C–H4C...O12	0.93	2.20	3.043(9)	151.1
O41–H41...O23	0.84	2.22	2.85(2)	132.7
N3–H3F...O21	0.91	2.45	3.045(9)	123.0
N3–H3D...O22	0.91	2.69	3.147(9)	111.7

[a] Symmetry transformations used to generate equivalent atoms: #1: $-x+1/2, y-1/2, -z+1/2$; #2: $-x+1/2, -y+3/2, -z$.

N4–C1, 1.156(8) Å (approximately triple) and one long C1–N5 1.323(9) Å (approximately single) bond within the 1,3-bridging entity. The irregular six-coordinate site involves the effectively singly-bonded C–N donor, which makes the smaller ($\approx 120^\circ$) C–N–Cu bridge angle. The cyanamide link is thus less colinear (Cu1–N4–C1 and C1–N5–Cu2 angles of $161.4(5)^\circ$ and $117.4(6)^\circ$, respectively) with respect to the pair of Cu^{II} paramagnets than the HNCN– bridge. The separation of the paramagnetic Cu^{II} ions is 6.133(2) Å. As usual in this cryptand system, there are intermolecular π – π contacts of the order (3.46 to 3.78 Å) of van der Waals distance.

Magnetic susceptibility and EPR measurements: The magnetic susceptibility of the hydrogencyanamido-bridged cryptate **1** was studied at a field of 1 T over the temperature range 2–250 K. The $\chi_M T$ versus T plot (Figure 3) shows the $\chi_M T$ values to increase with decreasing temperature to a maximum value of $1.029 \text{ cm}^3 \text{ K mol}^{-1}$ at 7 K and subsequently to decrease to a value of $0.997 \text{ cm}^3 \text{ K mol}^{-1}$ at 2 K. The experimental values can be fitted to a modified Bleaney–Bowers expression^[22] for the magnetic susceptibility of isotropically coupled $S=1/2$ dinuclear compounds, derived from the Hamiltonian $\mathbf{H} = -\mathbf{J}\cdot\mathbf{S}_1\cdot\mathbf{S}_2$: $\chi = [2N\gamma^2\beta^2/k(T-\theta)]\{\exp(-J/kT)\}$. The Weiss θ parameter was introduced in the formula to take into account possible antiferromagnetic interactions between dinuclear molecules together with zero-field splitting in the $S=1$ ground state. The results of the best fit, shown as the solid line in Figure 3 were $J=19.9(3) \text{ cm}^{-1}$, $g=2.03(1)$, $\theta=-0.07(1) \text{ K}$, showing a moderate ferromagnetic coupling. This coupling is of the same sense although larger size than that found in the colinear azido analogue ($J=7.5 \text{ cm}^{-1}$).^[23,24] The moderately strong antiferromagnetic interaction in the bis(1,3- μ -HNCN)dicopper(II) complex reported earlier^[7a] (bridge angles Cu–N–C ≈ 121 – 126° and 144 – 147°), implied by the 298 K moments of $1.35 \mu_B$ (298 K) and $0.66 \mu_B$ (98 K), respectively, is comparable with the level of antiferromagnetic interaction mediated by similarly bent azido bridges.^[3]

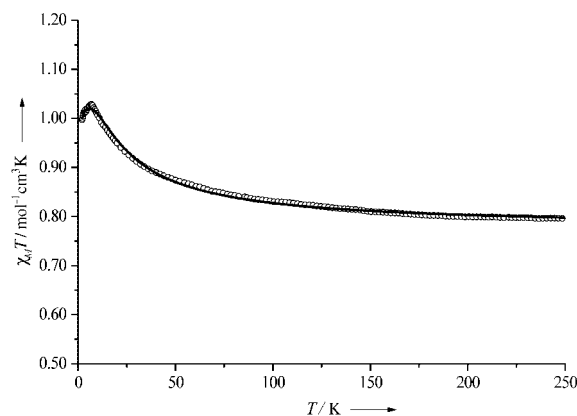


Figure 3. Plot of $\chi_M T$ versus T for compound **1**. The full line represents the best theoretical fit.

Another similarity with the azido analogues is demonstrated by the ESR spectrum of **1**, which confirms the existence of a triplet ground state in the range 4–298 K for the polycrystalline solid. Although the signals are broad (Figure 4), the spectrum possesses many of the features seen in azido analogues,^[14–16] including a pair of broad g_\perp and g_\parallel features, separated by zero-field splittings complicated by

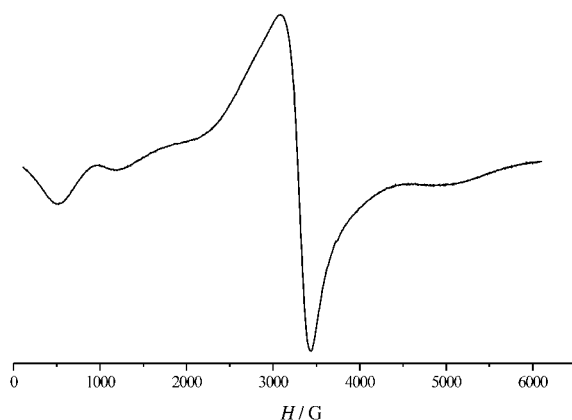


Figure 4. 298 K polycrystalline ESR spectrum of compound **1**.

overlapping of the low-field D_{\parallel} component feature with the half-band $\Delta M=2$ transition.

The magnetic susceptibility of the cryptates **2** and **3** was studied at a field of 1 T over the temperature range 2–300 K. The $\chi_M T$ versus T plot (Figure 5) indicates that the $\chi_M T$ values increase with decreasing temperature to maxima of $0.931 \text{ cm}^3 \text{ K mol}^{-1}$ at 9 K for **2** and $0.972 \text{ cm}^3 \text{ K mol}^{-1}$ at 5.5 K for **3**. The lowest values obtained are 0.772 and $0.914 \text{ cm}^3 \text{ K mol}^{-1}$ at 2 K for **2** and **3**, respectively. The experimental values can be fitted as in the case of **1** to the modified Bleaney–Bowers expression. The results of the best fit, shown as the solid lines in Figure 5, were $J=9.9(1) \text{ cm}^{-1}$, $g=2.08(1)$, $\theta=-0.79(1)$ and $J=7.5(1) \text{ cm}^{-1}$, $g=2.12(1)$, $\theta=-0.57(1) \text{ K}$ for **2** and **3**, respectively, indicating moderate ferromagnetic couplings.

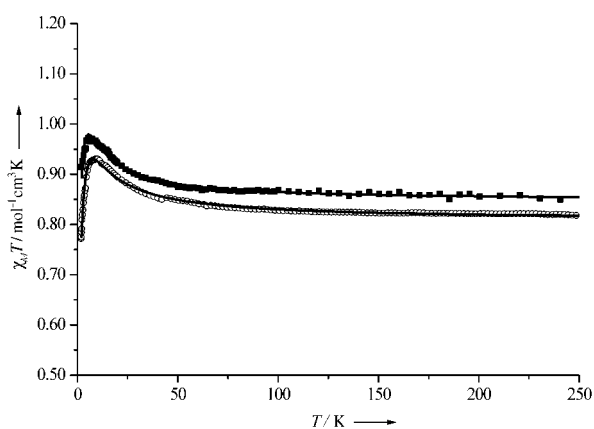


Figure 5. Plot of $\chi_M T$ versus T for compounds **2** ■ and **3** ○. The full lines represent the best theoretical fits.

The X-band ESR spectrum of **3** (Figure 6) exhibits sharper signals than that of compound **1** and provides confirmation of a triplet ground-state configuration,^[24] resembling that of the analogous azides.^[25,26] The most intense transi-

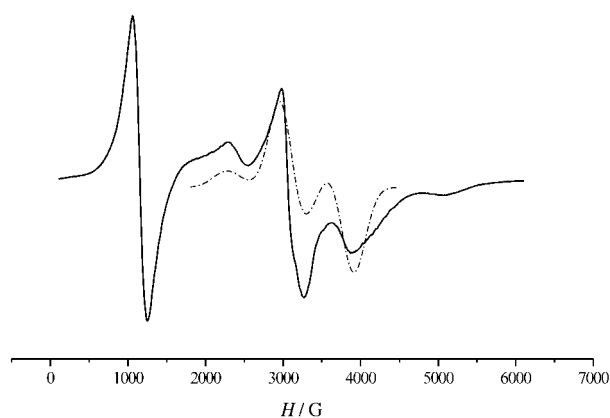


Figure 6. 4 K polycrystalline ESR spectrum of compound **3**. Dotted line shows the simulated triplet spectrum.

tion, presumably attributable to the forbidden half-band $\Delta M=2$ transition, appears around 1055 G, while pairs of peaks deriving from a zero-field splitting D of 800 G (as is shown in the simulation of Figure 6).

Electronic structure calculations: To understand the origin of the ferromagnetic coupling and the relative strength of the interaction, we have performed calculations using the B3LYP functional (see computation details in the Experimental Section). The calculated J constants for complexes **1** and **3** are $+18.7$ and $+12.9 \text{ cm}^{-1}$, respectively, in excellent agreement with the values of $+19.9$ and $+7.5 \text{ cm}^{-1}$ found experimentally. The spin density maps corresponding to the triplet states of such complexes are represented in Figure 7.

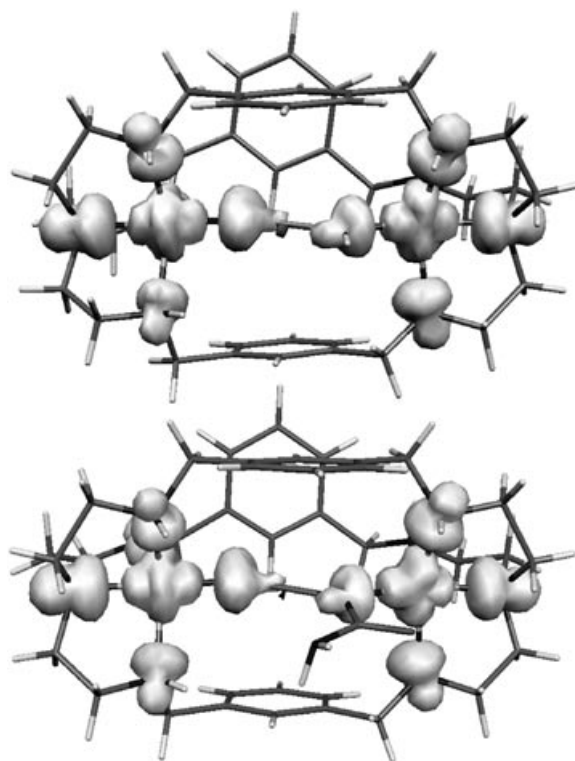


Figure 7. Representation of the spin density map calculated a B3LYP level for the complexes for complexes **1** (above) and **3** (below) (clear and dark regions indicate positive and negative spin populations, respectively).

The analysis of the spin density distribution shows the predominance for both complexes of a delocalisation mechanism in the nitrogen atoms coordinated to the copper atoms.^[27] It is worth noting the different shape of the spin density distribution due to the trigonal-bipyramid coordination of one of the copper atoms, whilst an axially elongated planar pyramid is adopted for the other copper atom. Small negative values of the spin density are found in the carbon atom of the bridging ligand, indicating a polarisation mechanism. In such cases, the odd number of atoms in the bridging

ligands favours the presence of a ferromagnetic interaction between the paramagnetic centres.

To explain the stronger ferromagnetic coupling of the hydrogencyanamido complex **1**, we have analysed the energies of the SOMOs corresponding to the triplet states of the two studied complexes (see Figure 8).^[28] The energy gap is rela-

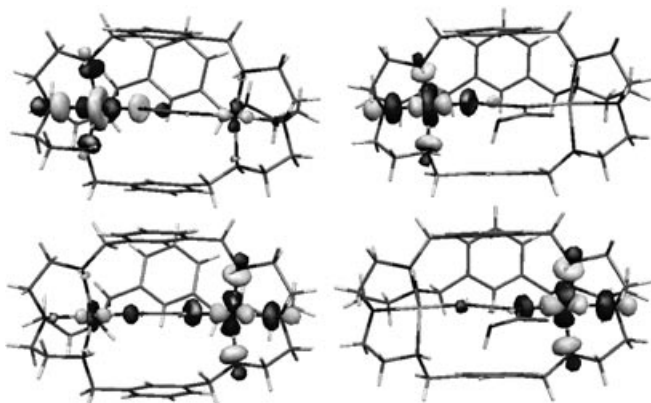


Figure 8. Representation of the SOMOs corresponding to the triplet states calculated a B3LYP level for the complexes **1** (left) and **3** (right).

tively small in both cases, in agreement with the ferromagnetic behaviour, being 0.08 eV for the hydrogencyanamido complex **1** and 0.30 eV for **3**. Hence a stronger ferromagnetic coupling would be expected for the complex **1**, as found experimentally. The origin of such difference cannot be attributed to the different nature of substituents of the cyanamido-bridging ligand, because the contribution of such substituents is almost negligible, as can be observed in Figure 8. The main structural differences between these two complexes are the larger bond lengths in the complex **3**, probably due to the steric effects of the amido substituent. For instance, the Cu–N bond length closer to the lower bond order C–N bond is 2.044 Å for the complex **3** and 1.968 Å for **1**. To check the influence of such structural parameters, we repeated the calculation of the exchange coupling constant for the complex **1**, modifying the structure to have the same Cu–N bond lengths in the bridging ligand as in complex **3**, obtaining a value of +13.8 cm⁻¹. This value is relatively close to the result obtained for the complex **3** (+12.9 cm⁻¹), indicating that such structural changes in the geometry of the bridging ligand may be considered responsible for the stronger ferromagnetic coupling in complex **1**.

Conclusion

In the present work, we have used dicopper cryptates as hosts for hydrogencyanamido ions and related species to generate 1,3-NCN-bridged cascade complexes. Starting from CaNCN and Na(NCNCN) we have prepared three new compounds, namely [Cu₂(HNCN)(R3Bm)](ClO₄)₃ (**1**), [Cu₂(dca)(R3Bm)](ClO₄)₃·4H₂O (**2**), and [Cu₂(NCN-

CONH₂)(R3Bm)](CF₃SO₃)₃ (**3**) (R3Bm = N[(CH₂)₂NHCH₂-(C₆H₄-*m*)CH₂NH(CH₂)₂]₃N; dca = dicyanamido ligand (NCNCN⁻)). For complexes **1** and **3**, X-ray diffraction analyses confirm the existence of a 1,3-cyanamido bridge. In compound **3** hydrolysis of the nitrile to amide, explained as cascade reactivity, is observed. All three compounds exhibit ferromagnetic coupling. The observation in three different complexes, which incorporate the 1,3-cyanamido bridge, of sizeable ferromagnetic interaction between the Cu^{II} paramagnets is striking and suggests a major role for this 1,3-pathway in explaining the ferromagnetically ordered behaviour seen in many dicyanamido bridged complexes. Theoretical calculations demonstrate the importance of geometry, especially Cu^{II}–N distances, and in particular the significant influence of the more singly bonded N–Cu contact on the size of the interaction mediated. This suggests that careful tuning of this distance by means of host-molecule design may enable observation of larger ferromagnetic couplings between pairs of Cu^{II} ions or other paramagnets.

Experimental Section

The ligand R3Bm was made as previously described.^[29]

Caution: Perchlorate salts of transition-metal complexes are hazardous and may explode. Only small quantities should be prepared and great care should be taken.

[Cu₂(HNCN)(R3Bm)](ClO₄)₃ (**1**): We added Cu(ClO₄)₂·6H₂O (74.1 mg, 0.2 mmol) dissolved in a mixture of MeCN (5 mL) and EtOH (3 mL) to a solution of the cryptand (61.2 mg, 0.1 mmol) in MeOH (3 mL). An excess of CaNCN (12.0 mg, 0.15 mmol) was added to this solution, and the mixture was stirred at room temperature for 3 h, during which time a green precipitate appeared. This green solid was recrystallised by using vapor diffusion of MeOH into a solution of the solid in acetonitrile. The crystals obtained in 62.9% yield were suitable for X-ray crystallography. Elemental analysis calcd (%): C 41.7, H 5.2, N 13.1; found: 41.3, H 5.3, N 12.9; FAB-MS clusters (run on the more soluble triflate salt) *m/z* (%): 659 [Cu(R3Bm)]⁺ (45), 873 [Cu₂(R3Bm)(CF₃SO₃)₃]⁺ (100), 1065 [Cu₂(R3Bm)NCNH(CF₃SO₃)₂]⁺ (85); Selected IR data (perchlorate salt): $\tilde{\nu}$ = 3264 (ms; NH), 3231 (ms; NH), 3224 (ms; NH), 2219 (ms; HNCN⁻), 1089 (vs; counterion), 625 cm⁻¹ (ms; counterion).

[Cu₂(dca)(R3Bm)](ClO₄)₃·4H₂O (**2**): R3Bm (61.2 mg, 0.1 mmol) was dissolved in MeOH (3 mL); then Cu(ClO₄)₂·6H₂O (75.0 mg, 0.2 mmol) in a mixture of MeCN (2 mL) and EtOH (3 mL) was added. Finally we added solid Na[N(CN)₂] (10.3 mg, 0.10 mmol), which rapidly dissolved. After a few minutes stirring we observed the formation of a bright blue precipitate in 82.1% yield. This product was too insoluble for recrystallisation or for FAB-MS. Elemental analysis calcd (%): C 39.3, H 5.4, N 13.3; found: C 39.0, H 5.3, N 13.1; Selected IR data: $\tilde{\nu}$ = 3319 (w; NH), 3307 (mw; NH), 3294 (w; NH), 3252 (w; NH) 2214 (mw; NCNCN⁻), 2193 (ms; NCNCN⁻), 2140 (w; NCNCN⁻), 1095 (vs; counterion), 624 cm⁻¹ (ms; counterion).

[Cu₂(NCNCONH₂)(R3Bm)](CF₃SO₃)₃ (**3**): We added Cu(CF₃SO₃)₂ (73.8 mg, 0.2 mmol) dissolved in a mixture of CH₃CN (5 mL) and EtOH (2 mL) to a solution of R3Bm (61.7 mg, 0.1 mmol) in MeOH (3 mL); this was followed by the addition of Na[N(CN)₂] (13.1 mg, 0.15 mmol) as a solid. After several minutes stirring, the solution was filtered and allowed to evaporate slowly to dryness. The resulting solid was treated with MeCN/EtOH (5 mL:1 mL) and filtered. The blue solution was allowed to evaporate slowly and a blue crystalline solid suitable for X-ray crystallography was obtained in 5.2% yield. Elemental analysis calcd (%): C 39.2, H 4.5, N 12.3; found: C 38.5, H 4.5, N 12.1; Selected IR data: $\tilde{\nu}$ = 3248

(ms; NH₃), 2228 (ms; NCN), 1663 (ms; CO); 1253 (counterion), 1164 (counterion), 1031 cm⁻¹ (counterion).

Physical measurements: IR spectra were measured on Nicolet 520 FTIR spectrophotometers as KBr pellets. Magnetic susceptibilities were measured on polycrystalline powders at the Servei de Magnetoquímica of the Universitat de Barcelona with a Quantum Design SQUID MPMS-XL susceptometer working in the range 2–300 K under magnetic fields of approximately 1 T. Diamagnetic corrections were estimated from Pascal constants. EPR spectra were recorded with a Bruker ES200 spectrometer at X-band frequency.

X-ray crystallography: Details of data collection and refinement are given in Table 3. Data were collected on a Bruker SMART 1000 diffractometer, the structures were solved by direct methods and refined by

Table 3. Crystallographic data for complexes [Cu₂(R3BM)(NCN)]-(ClO₄)₃·MeCN·MeOH (**1**·MeCN·MeOH) and [Cu₂(R3Bm)(NCN·CONH₂)](CF₃SO₃)₃·0.5 EtOH·0.5 H₂O (**3**·0.5 EtOH·0.5 H₂O).

	1 ·MeCN·MeOH	3 ·0.5 EtOH·0.5 H ₂ O
formula	C ₄₀ H ₆₂ Cl ₃ Cu ₂ N ₁₁ O ₃	C ₄₂ H ₆₀ Cu ₂ F ₉ N ₁₁ O ₁₁ S ₃
M _r	1138.44	1289.27
crystal system	monoclinic	monoclinic
a [Å]	15.4163(11)	31.179(3)
b [Å]	12.2826(9)	16.6111(16)
c [Å]	27.0219(19)	21.408(2)
β [°]	102.646(1)	96.051(2)
V [Å ³]	4992.5(6)	535.7(3)
Z	4	8
space group	P2 ₁ /n	C2/c
μ [mm ⁻¹]	1.084	0.980
reflms collected	47727	26606
unique reflms (R _{int})	8814 (0.0499)	7931 (0.0635)
R1/wR2 [I > 2σ(I)] ^[a,b]	0.0550/0.1508	0.0698/0.1856
R1/wR2 (all data) ^[a,b]	0.0781/0.1742	0.1080/0.2227

[a] $R1 = \sum(|F_o| - |F_c|) / \sum(F_o)$. [b] $wR2 = \{\sum[w((F_o - F_c)^2) / \sum(w(F_o)^2)]\}^{1/2}$, $w = 1/[\sigma^2(F_o^2) + (aP)^2 + bP]$ and $P = [2F_c^2 + \text{Max}(F_o^2, 0)]/3$.

full-matrix least-squares on F^2 using all the data. All programs used in structure solution and refinement are included in the SHELXTL package.^[30] All non-hydrogen atoms were refined with anisotropic atomic displacement parameters and hydrogen atoms were included at calculated positions using a riding model except for those described below:

[Cu₂(R3BM)(HNCN)](ClO₄)₃·MeCN·MeOH: The asymmetric unit contained one molecule of acetonitrile and two half-occupancy methanol solvate molecules; the amine protons were located from difference maps. There was some residual electron density around one of the methanol solvate molecules, but this was not modelled.

[Cu₂(R3Bm)(NCNCONH₂)](CF₃SO₃)₃·0.5 EtOH·0.5 H₂O: Hydrogen atoms bound to the primary amine in the bridging group were inserted as 2/3 occupancy of the three sp³ positions, while those bound to partial occupancy oxygen atoms were not located or included in the refinement. There were a few significant peaks in the difference map suggestive of some disorder of the tren-derived caps, possibly connected with the observation that one of the cryptand strands had a different conformation to the others. No attempt was made to model this very minor disorder. CCDC 241786 and 241787 contain the supplementary crystallographic data for this paper. These data can be obtained free of charge via www.ccdc.cam.ac.uk/conts/retrieving.html (or from the Cambridge Crystallographic Data Centre, 12 Union Road, Cambridge CB2 1EZ, UK; fax: (+44)1223-336-033; or e-mail: deposit@ccdc.cam.ac.uk).

Computational details: The hybrid density functional B3LYP^[31–33] with the broken-symmetry approach provided good numerical estimates of the exchange coupling constant J (introduced by the phenomenological Heisenberg Hamiltonian $H = -J\cdot S_1\cdot S_2$)^[34,35] by using the GAUSSIAN package and an all-electron basis set.^[36] The use of the nonprojected energy

of the broken symmetry solution as the energy of the low-spin state within the DFT framework provided good results, because it avoided the cancellation of the nondynamic correlation effects as stated recently by works of Kraka and the Cremer group.^[37,38] The details of the methodology employed were discussed in detail in a previous report.^[39,40] We employed a triple- ζ all-electron basis set that included two p polarisation functions for the copper atoms^[41] and a double- ζ all-electron for the other elements^[42] proposed by Ahlrichs et al.

Acknowledgements

This research was partially supported by CICYT (Grants BQU2003/0538 and BQU2002-04033-C02-01). We are grateful to EPSRC mass spectrometry service in Swansea.

- [1] J. L. Burmeister, *Coord. Chem. Rev.* **1990**, *105*, 77–133.
- [2] J. Ribas, A. Escuer, M. Montfort, R. Vicente, R. Cortes, L. Lezama, T. Rojo, *Coord. Chem. Rev.* **1999**, *193*, 1027–1068.
- [3] a) O. Kahn, *Molecular Magnetism*, VCH, **1993**; b) A. Escuer, M. Font-Bardía, S. S. Massoud, F. A. Mautner, E. Peñalba, X. Solans and R. Vicente, *New J. Chem.* **2004**, *28*, 681–686.
- [4] V. McKee, J. V. Dagdigian, R. Bau, and C. A. Reed, *J. Am. Chem. Soc.* **1981**, *103*, 7000–7001.
- [5] a) M. G. B. Drew, C. J. Harding, J. Nelson, *Inorg. Chim. Acta* **1996**, *246*, 73–79; b) E. Ruiz, J. Cano, S. Alvarez, P. Alemany, *J. Am. Chem. Soc.* **1998**, *120*, 11 122–11 129; c) A. Escuer, M. A. S. Goher, F. A. Mautner, R. Vicente, *Inorg. Chem.* **2000**, *39*, 2107–2112.
- [6] A. Escuer, C. J. Harding, Y. Dussart, J. Nelson, V. McKee, R. Vicente, *J. Chem. Soc. Dalton Trans.* **1999**, 223–228.
- [7] a) P. Chaudhuri, K. Wieghardt, B. Nuber, J. Weiss, *J. Chem. Soc. Chem. Commun.* **1985**, 265–266. b) F. Meyer, I. Hyla-Kryspin, E. Kaifer, P. Kircher, *Eur. J. Inorg. Chem.* **2000**, *4*, 771–781.
- [8] S. R. Batten, K. S. Murray, *Coord. Chem. Rev.* **2003**, *246*, 103–130.
- [9] Z.-M. Wang, B.-W. Sun, J. Luo, S. Gao, C.-S. Liao, C.-H. Yan, Y. Li, *Inorg. Chim. Acta* **2002**, *332*, 127–134.
- [10] R. J. Crutchley, *Coord. Chem. Rev.* **2001**, *219*, 125–155.
- [11] M. L. Brader, E. W. Ainscough, E. N. Baker, A. M. Brodie and S. L. Ingham, *J. Chem. Soc. Dalton Trans.* **1990**, 2785–2792.
- [12] a) A. Escuer, N. Sanz, R. Vicente, F. A. Mautner, *Inorg. Chem.* **2003**, *42* 541–55. b) A. Escuer, F. A. Mautner, N. Sanz, R. Vicente, *Dalton Trans.* **2003**, 2121–2125; c) A. Escuer, N. Sanz, F. A. Mautner, R. Vicente, *Eur. J. Inorg. Chem.* **2004**, 309–316.
- [13] Y. Dussart, C. Harding, P. Dalgaard, C. McKenzie, R. Kadriavelraj, V. McKee, J. Nelson, *J. Chem. Soc. Dalton Trans.* **2002**, 1704–1713.
- [14] J. Nelson, V. McKee, G. Morgan, *Prog. Inorg. Chem.* **1998**, *47*, 167–316.
- [15] M. Kuhn, R. Mecke, *Chem. Ber.* **1961**, *94*, 3016–3022.
- [16] a) Q. Lu, J.-M. Latour, C. J. Harding, N. Martin, D. J. Marrs, V. McKee, J. Nelson, *J. Chem. Soc. Dalton Trans.* **1994**, 1471–1479; b) C. J. Harding, Q. Lu, D. J. Marrs, N. Martin, V. McKee, J. Nelson, *J. Chem. Soc. Dalton Trans.* **1995**, 1739–1747.
- [17] a) J.-M. Lehn, *Pure Appl. Chem.* **1980**, *52*, 2441–2459; b) J.-M. Lehn, *Science* **1985**, *227*, 849–856.
- [18] R. Boca, M. Hvastijová, J. Kosísek, M. Valkó, *Inorg. Chem.* **1996**, *35*, 4794–4797.
- [19] T. Lu, X. Zhuang, Y. Li, S. Chem, *J. Am. Chem. Soc.* **2004**, *126*, 4760–4761.
- [20] A. Bond, J. Nelson, S. Derossi, unpublished results.
- [21] a) A. W. Addison, T. N. Rao, J. Reedijk, J. van Rijn, and G. C. Verschoor, *J. Chem. Soc. Dalton Trans.* **1984**, 1349–1356; b) R. S. Berry, *J. Chem. Phys.* **1960**, *32*, 933–938.
- [22] B. W. Bleaney, K. D. Bowers, *Proc. R. Soc. London Ser. A* **1952**, *214*, 451–465.
- [23] M. G. B. Drew, J. Hunter, D. J. Marrs, J. Nelson, C. Harding, *J. Chem. Soc. Dalton Trans.* **1992**, 3235–3243.

- [24] C. J. Harding, F. E. Mabbs, E. J. L. Mc Innes, V. McKee, J. Nelson, *J. Chem. Soc. Dalton Trans.* **1996**, 3227–3230.
- [25] J. Reedijk, B. Nieuwenhuijse, *Recl. Trav. Chim. Pays Bas*, **1972**, *91*, 533–551.
- [26] F. E. Mabbs, D. Collinson, *EPR of Transition metal compounds*, Elsevier, Amsterdam, **1992**, Chapter 11.
- [27] J. Cano, E. Ruiz, S. Alvarez, M. Verdaguier, *Comments Inorg. Chem.* **1998**, *20*, 27–56.
- [28] P. J. Hay, J. C. Thibeault, R. Hoffmann, *J. Am. Chem. Soc.* **1975**, *97*, 4884–4899.
- [29] C. J. Harding, Q. Lu, J. F. Malone, D. J. Marrs, N. Martin, V. McKee, J. Nelson, *J. Chem. Soc. Dalton Trans.* **1995**, 1739–1743.
- [30] G. M. Sheldrick, SHELXTL Version 6.12, Bruker AXS, Madison WI, **2001**.
- [31] A. D. Becke, *Phys. Rev. A* **1988**, *38*, 3098–3100.
- [32] A. D. Becke, *J. Chem. Phys.* **1993**, *98*, 5648–5652.
- [33] C. Lee, W. Yang, R. G. Parr, *Phys. Rev. B* **1988**, *37*, 785–789.
- [34] E. Ruiz, P. Alemany, S. Alvarez, J. Cano, *J. Am. Chem. Soc.* **1997**, *119*, 1297–1303.
- [35] E. Ruiz, S. Alvarez, A. Rodríguez-Forteza, P. Alemany, Y. Pouillon, C. Massobrio, in *Magnetism: Molecules to Materials, Vol. 2* (Eds.: J. S. Miller, M. Drillon), Wiley-VCH, Weinheim, **2001**, p. 227.
- [36] Gaussian98 (Release A.11) M. J. Frisch, G. W. Trucks, H. B. Schlegel, G. E. Scuseria, M. A. Robb, J. R. Cheeseman, V. G. Zakrzewski, J. A. Montgomery, R. E. Stratmann, J. C. Burant, S. Dapprich, J. M. Millam, A. D. Daniels, K. N. Kudin, M. C. Strain, O. Farkas, J. Tomasi, V. Barone, M. Cossi, R. Cammi, B. Mennucci, C. Pomelli, C. Adamo, S. Clifford, J. Ochterski, G. A. Petersson, P. Y. Ayala, Q. Cui, K. Morokuma, D. K. Malick, A. D. Rabuck, K. Raghavachari, J. B. Foresman, J. Cioslowski, J. V. Ortiz, B. B. Stefanov, G. Liu, A. Liashenko, P. Piskorz, I. Komaromi, R. Gomperts, R. L. Martin, D. J. Fox, T. Keith, M. A. Al-Laham, C. Y. Peng, A. Nanayakkara, C. Gonzalez, M. Challacombe, P. M. W. Gill, B. G. Johnson, W. Chen, M. W. Wong, J. L. Andres, M. Head-Gordon, E. S. Replogle, J. A. Pople, Gaussian, Inc, Pittsburgh, PA, **1998**.
- [37] V. Polo, E. Kraka, D. Cremer, *Theor. Chem. Acc.* **2002**, *107*, 291–303.
- [38] V. Polo, J. Grafenstern, E. Kraka, D. Cremer, *Theor. Chem. Acc.* **2003**, *109*, 22–35.
- [39] E. Ruiz, J. Cano, S. Alvarez, P. Alemany, *J. Comput. Chem.* **1999**, *20*, 1391–1400.
- [40] E. Ruiz, A. Rodríguez-Forteza, J. Cano, S. Alvarez, P. Alemany, *J. Comput. Chem.* **2003**, *24*, 982–989.
- [41] A. Schaefer, C. Huber, R. Ahlrichs, *J. Chem. Phys.* **1994**, *100*, 5829–5835.
- [42] A. Schaefer, H. Horn, R. Ahlrichs, *J. Chem. Phys.* **1992**, *97*, 2571–2577.

Received: June 21, 2004
Published online: November 19, 2004